

Evaluation of Chitosan and Their Self-Assembled Nanoparticles with pDNA for the Application in Gene Therapy

Kishor Sarkar,¹ Rishi Srivastava,¹ Urmi Chatterji,² P. P. Kundu¹

¹Department of Polymer Science and Technology, University of Calcutta, Kolkata-9, India

²Department of Zoology, University of Calcutta, Kolkata-19, India

Received 24 November 2009; accepted 23 November 2010

DOI 10.1002/app.33832

Published online 16 March 2011 in Wiley Online Library (wileyonlinelibrary.com).

ABSTRACT: The molecular weight (MW) of chitosan (CS) was determined by viscometric method (using Mark-Houwink equation) as well as by gel permeation chromatography, and the degree of deacetylation (DDA) of CS was measured by potentiometric titration method and Gran-type linearization method. The values of DDA were obtained $\sim 83\%$ (by potentiometric titration method) and $\sim 86\%$ (by Gran-type linearization method). The self-assembled nanoparticles of CS/plasmid DNA (pDNA) complex were prepared by varying the concentration of CS. The formation of CS/pDNA complex was confirmed by 0.8% agarose gel electrophoresis and the particle size of the self-assembled nanoparticle was determined by dynamic light scattering, atomic force micros-

copy and scanning electron microscopy. The stability of CS/pDNA complexes was determined by turbidity test with the help of UV-Vis spectroscopy. The effect of ionic strength on the complexes was also observed by means of fluorescence spectroscopy. The cytotoxicity of CS on the HeLa cell line was observed by absorbance of MTT (3-(4,5-dimethylthiazol-2-yl)-2,5-diphenyltetrazolium bromide) assay and showed that CS has lower cytotoxicity in HeLa cells compared with that of poly(L-lysine) in 293T cells. © 2011 Wiley Periodicals, Inc. *J Appl Polym Sci* 121: 2239–2249, 2011

Key words: chitosan; nanoparticles; dynamic light scattering; DNase I

INTRODUCTION

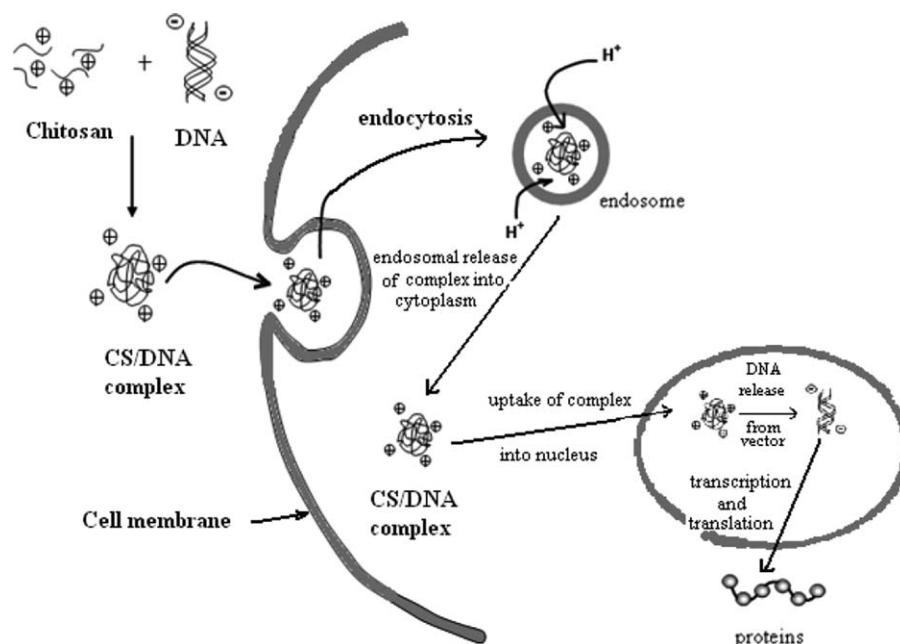
The basic concept of gene therapy is the introduction of a fresh gene into the specific cells of a patient to treat genetic diseases (Scheme 1) such as cancer,¹ AIDS,² Alzheimer,³ Parkinson's disease,⁴ and cardiovascular problems.⁵ However, there are lower success rate of gene therapy due to the lack of safe and efficient DNA carriers. Due to the several problems such as, high immunogenicity, risk of replication, random DNA insertion, and mass production⁶ of viral vectors, nonviral vectors for gene therapy have been increasingly proposed as safer alternatives to viral vectors.⁷ Nonviral vectors can be administered repeatedly with minimal host immune response and they are stable in storage and are easy to produce in large quantities. Currently, among the nonviral vectors, cationic lipids, and cationic polymers are the two strong candidates. Cationic lipids have several advantages over the viral vectors, but they have higher toxicity and lower transfection efficiency

compared with that of the viral vectors.⁸ Therefore, cationic polymers have gained more preference because they can easily form polyelectrolyte complex (called polyplex) with negatively charged pDNA through charge interaction and self-assembling.⁹ There are several cationic polymers that can be used for efficient gene expression, including poly(L-lysine),¹⁰ polyethyleneimine (PEI),¹¹ polyamidoamine dendrimers,¹² poly(phosphoramidate),¹³ and poly(β -amino ester).¹⁴ An ideal polymeric gene carrier should have higher gene transfer efficiency, targeting ability, and good biocompatibility. On the other hand, the polyplex should have high stability during lyophilization to ultimately apply genes like pharmaceuticals. PEI is accepted as one of the most efficient nonviral vector due to its higher transfection efficiency and higher density of primary and secondary amines, which help effective binding and compaction with pDNA.¹⁵ But, PEI exhibits higher cytotoxicity in most cases and its nonbiodegradability inhibits its clinical development.¹⁶

In recent years, several research groups have considered chitosan (CS) as a potential cationic polymer for gene carrier.^{17–21} CS is a good biocompatible, biodegradable polysaccharide²² and also is nontoxic both in experimental animals²³ and humans.²⁴ CS is a naturally occurring linear binary cationic polysaccharide

Correspondence to: P. P. Kundu (ppk923@yahoo.com).

Contract grant sponsor: Nanoscience and Nanotechnology, University of Calcutta.



Scheme 1 Graphical modeling of gene therapy.

consisting of D-glucosamine and N-acetyl-D-glucosamine repeating units linked by a β (1 \rightarrow 4) glycosidic bond (Fig. 1). CS is obtained by the deacetylation of chitin, which is obtained from crab and shrimp shells by chemical processing. Because of its good biocompatibility and toxicity profile, it has wide application in pharmaceutical field as a drug delivery carrier and also as biomedical material for artificial skin and wound healing bandage.²⁵ At acidic pH, the amine groups of CS become positively charged and can effectively bind with negatively charged DNA and condense it as nano/micro particles.²⁶ In the absence of serum, highest transfection is obtained in COS-1 cells with a 102-kDa CS/DNA complex at the charge ratio of 2 : 1.²⁷ Extensive efforts are being expended for improving new nonviral vehicles by using CS polymers. Several derivatives of CS have been prepared based on the reaction with free amine groups.²⁸ In a recent study, Kim et al.²⁹ prepared galactosylated CS to improve the transfection efficiency and targeting capability of CS/DNA nanoparticles. They showed that HepG2 (human hepatoblastoma cell line) having asialoglycoprotein receptors binding galactose containing ligands was more efficiently transfected than HeLa cells without asialoglycoprotein receptors.

It was also reported that lactocylated- CS/DNA complexes efficiently transfected HeLa cells, but not HepG2³⁰ cells. Mao et al.¹⁷ have also improved the transfection efficiency by 130-fold in HeLa cells by conjugated KNOB (C-terminal domain of the fiber protein of adenoviruses) to CS/DNA nanoparticles.

Analogous to molecular weight (MW) of CS, the degree of deacetylation (DDA) of CS is a complex factor influencing the transfection efficiency in gene therapy. The presence of N-acetyl groups on the CS backbone imparts hydrophobic property, which renders CS for self-aggregation in aqueous solution,³¹ probably affecting the interaction of CS and DNA. Therefore, it is necessary to know the DDA value of CS. Leong's group³² observed the effect of the DDA of CS on the level of transfection efficiency. They found that the gene expression level in presence of serum decreased upon reducing DDA, which is supposed to lower the stability of complexes.

The physicochemical properties of CS/DNA complexes are necessary for successful gene therapy, although a lot of modification of CS carried out to improve the transfection efficiency.

In this work, we characterized the CS and investigated the physicochemical properties of CS/pDNA

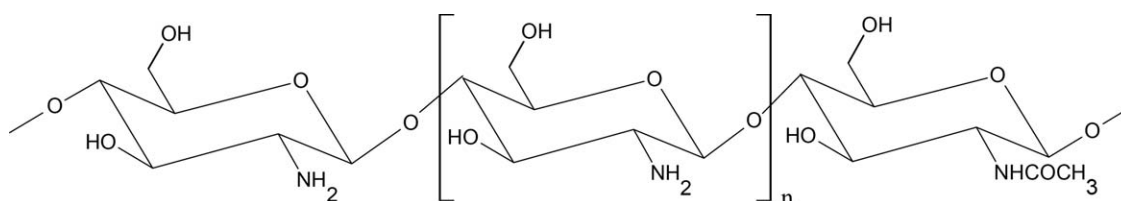


Figure 1 Structure of CS.

complexes by means of dynamic light scattering (DLS) method, fluorescence spectroscopy, atomic force microscopy (AFM), and scanning electron microscopy (SEM) for successful gene therapy.

EXPERIMENTAL

Materials

CS (MW-563 kDa and DDA-86%) was purchased from Tokyo Kasei Kogyo, Japan. DNase I (1 unit/ μ L), sodium sulfate, ethidium bromide, *N*-2-hydroxyethyl-piperazine-*N*-2-ethanesulfonic acid (HEPES), and MTT were purchased from Sigma-Aldrich. Dipalmitoyl-*sn*-glycero-3-phosphocholine (DPPC) in powder form, Dulbecco's modified eagle medium (DMEM) and fetal bovine serum (FBS) were obtained from Gibco. pGL3-control vector (5.25 kb) containing SV-40 promoter, resulting in strong expression of luc⁺, was purchased from Promega (Madison, WI). All other reagents were analytical grade and were used directly without further modification.

Determination of molecular weight of chitosan

CS was purified by reprecipitation method. It was dissolved in 1% acetic acid solution with constant stirring by a magnetic stirrer and then, the CS was reprecipitated by the addition of 4*N* sodium hydroxide solution. The precipitate was washed with distilled water until the pH became neutral and finally, it was washed with ethanol. The purified CS was then dried under vacuum overnight at 55°C. The MW was determined by this purified CS. The MW of CS was measured by viscometric method using the well-known Mark-Houwink equation:

$$[\eta] = \kappa \bar{M}_V^\alpha \quad (1)$$

where $[\eta]$ is intrinsic viscosity, κ and α are constants, and \bar{M}_V is viscosity average MW. The values of κ and α depend on the polymer type, solvent, and temperature.

The intrinsic viscosity of CS was measured with Ubbelohde viscometer in 0.5*M* acetic acid/0.2*M* sodium acetate solution at $25 \pm 1^\circ\text{C}$. As reported in Ref.³³, the values of the constants κ and α for CS and the solvent 0.5*M* acetic acid/0.2*M* sodium acetate are 3.5×10^{-4} and 0.76, respectively, and they do not depend on the deacetylation degree of CS.

The MW of CS was also determined by gel permeation chromatography (GPC). The GPC equipment consisted of ultrahydrogel 1000 (7.8 \times 300 mm) column, 515 HPLC pump and 2414 RI detector (Waters, USA). The mobile phase was 0.1*M* acetic acid/0.1*M* sodium acetate buffer. Mobile phase and CS solution were filtered through 0.45 μm filter (Millipore). The

flow rate was maintained at 0.3 mL/min. The sample concentration was 0.3 mg/mL. Polyethylene glycol (Sigma-Aldrich) standards were used to calibrate the column. All data provided by the GPC system were analyzed using the Empower 2 software package.

Determination of degree of deacetylation of chitosan

The DDA of CS was determined by the potentiometric titration method. The pH of the solution during the whole titration process was measured by a lab pH meter (Make- CD, India, Model: APX175 E/C). We followed the method of Chebotok et al.³³ with slight modification. Briefly, 0.1 g of purified CS was accurately weighed (± 0.0001 g) and dissolved in a 10 mL of 0.1*M* HCl solution with constant stirring and kept for 24 h for complete dissolution of the CS and then, calculated amount of sodium chloride was added to adjust the ionic strength to 0.1. The resulting solution was titrated with 0.1*M* NaOH solution containing 0.1*M* NaCl. At first, the NaOH solution was added to the CS solution with constant stirring until the pH of the solution reached at 2.0. Then, the standard NaOH solution was added stepwise and 0.2 mL solution was added in each step. The resulting pH and the added volume of NaOH solution were recorded during the whole titration process. The DDA of CS was calculated by two ways: (1) by potentiometric titration method³⁴ and (2) by Gran-type linearization method.³⁵ In the potentiometric titration method, the titration curve of pH versus volume of NaOH (mL) was plotted. Then, the points of the maxima of the first derivative, which corresponded to the equivalence point of the excess HCl (V_1) and protonated amino groups (V_2), were determined.

In the potentiometric titration method, the DDA (%) of CS was calculated by using the following equation:

$$DDA(\%) = \frac{203.2}{42.0 + \frac{1000m}{c_{\text{NaOH}}(V_2 - V_1)}} \times 100 \quad (2)$$

where m is the amount of CS (g) in the solution, c_{NaOH} is the concentration of NaOH solution (*M*), $V_2 - V_1$ is the volume of NaOH solution consumed in titration of amino groups of CS, 203.2 is the MW of the acetylated monomeric unit of the polysaccharide, 42.0 is the difference between the MWs of the deacetylated monomeric unit and acetylated monomeric unit, 1000 is the conversion factor of milliliters to liters and 100 is the conversion factor of DDA to percents.

In the Gran-type linearization method, the titration was carried out until the pH reached a value of 5.

The DDA (%) of CS was determined by using the following equation:

$$DDA(\%) = \frac{d}{\frac{W-161d}{204} + d} \times 100 \quad (3)$$

$$d = \frac{C_1 V_1 - C_B V_e}{1000} \quad (4)$$

where C_1 is the concentration of HCl aqueous solution (M), V_1 is the volume of HCl solution (mL), C_B is the concentration of NaOH solution (M), V_e is the volume of NaOH at the end point of the titration (mL), 204 is the MW of the acetylated monomeric unit of the polysaccharide, 161 is the MW of the deacetylated monomeric unit of the polysaccharide, and W is the weight of sample (g).

To calculate the value of V_e , a value of $f(x)$, the corresponding volume of NaOH added during the titration was calculated by using the following equation:

$$f(x) = \left(\frac{V_0 + V}{C_B} \right) \times ([H^+] - [OH^-]) \quad (5)$$

where V_0 is the volume of CS solution (mL), V is the volume of NaOH added (mL), $[H^+]$ is the concentration of H^+ (M), and $[OH^-]$ is the concentration of OH^- (M). The linear titration curve was obtained by plotting $f(x)$ versus the corresponding volume of NaOH solution. The value of V_e was determined by extrapolating the linear titration curve to the x -axis.

Preparation of plasmid DNA

The plasmids were propagated in *Escherichia coli* and isolated by the Qiagen Plasmid Purification Midi Kit (Qiagen, Chatsworth, CA). The isolated pDNA was washed with 70% ethanol at room temperature, air dried for 5–10 min and then, resuspended in distilled water. The purity and concentration of DNA was determined by measuring UV absorbance at 260 and 280 nm. The obtained pDNA was stored at -20°C for further use.

Preparation of CS/pDNA complex

The purified CS was again dissolved in 1% acetic acid solution under constant stirring for 30 min and then, the pH of the solution was adjusted at 5.5–5.7 by the addition of sodium hydroxide solution. pDNA was dissolved (10 $\mu\text{g}/\text{mL}$) in 25 mM of sodium sulfate solution. Both the CS and DNA solutions were preheated separately at 50–55 $^\circ\text{C}$ for 10 min. Then, CS/pDNA complexes at various charge ratios (amino group to phosphate ratio, N/P) were prepared by immediately mixing of equal volume of CS and pDNA solution and subsequently vortexing

for 15–30 s with cyclomixer (REMI, India). Then, the mixtures were incubated at room temperature for 30 min to completely form the CS/pDNA complexes.

Gel electrophoresis shift assay

The binding ability of CS with pDNA was determined by agarose gel electrophoresis. Agarose gel (0.8%, w/v) was prepared in TAE buffer (40 mmol/L Trisacetate and 1 mmol/L EDTA) and ethidium bromide (10 $\mu\text{g}/\text{mL}$) was added to the gel as a DNA visualizer. Then, the samples with different N/P ratios were loaded in the gel for electrophoresis. The gel electrophoresis was carried out at 100 V for 30 min and then, the gel was illuminated on an UV illuminator to show the location of the pDNA. The picture of the gel was subsequently captured by BIO-RAD gel doc system.

Determination of particle size and zeta potential by dynamic light scattering

The particle sizes and distributions as well as surface charge of CS/pDNA complexes at different N/P ratios were determined by the help of DLS. The DLS measurement was carried out by means of an argon ion laser system tuned at 514 nm. To avoid the influence of dust on the reliability of results, the solutions of the CS/pDNA complex were filtered through a 0.5- μm filter (Millipore) directly into a freshly cleaned 10 mm diameter cylindrical cell. The intensity of autocorrelation was measured at a scattering angle (θ) of 173 $^\circ$ with Zetasizer Nano ZS (Malvern Instrument, UK) digital autocorrelator at 37 $^\circ\text{C}$. The correlation function was accepted when the difference between the measured and the calculated baselines was less than 0.1%. The mean diameter was obtained by the Stokes–Einstein relationship.

Atomic force microscopy measurement

The size and morphology of CS/pDNA complexes were characterized by AFM (Nanoscope IV Bioscope, Digital Instruments, Veeco). One to two microliters of samples containing complexes in acetate buffer with a final DNA concentration of 100 $\mu\text{g}/\text{mL}$ was deposited onto the center of a freshly split untreated mica disk. The mica surface was dried at room temperature before imaging. The imaging was conducted with silicon nitride tip in tapping mode and a scan speed of 1 Hz at ambient condition.

Scanning electron microscopy measurement

The polymer/DNA complexes were prepared as described above. About 10 μL of complex suspension was deposited onto a glass slide. After drying

at room temperature, the morphology of the sample was observed by a scanning electron microscope (Hitachi, Japan, Model-3400N). Before the SEM observation, the samples were fixed on an aluminum stub and coated with gold by ion sputter coater (Hitachi, Japan, Model-E1010) for 7 min.

Turbidity measurement of CS/pDNA complex

For turbidity test, the CS/pDNA complexes with different N/P ratios were dispersed in 5 mM acetate buffer containing 25 mM sodium sulfate and sonicated using a sonicator at 30 W for 3 min. The stability of the complexes was evaluated by turbidity measurement using a UV-Vis spectrophotometer (UV-1700 Pharmaspec, Shimadzu, Japan) at 340 nm and at different time intervals.

Effect of ionic strength on CS/pDNA complex

pDNA (100 $\mu\text{g}/\text{mL}$) was stained with ethidium bromide (EtBr) in 1 mM Hepes buffer (pH 5.7) at a molar ratio of 10 : 1 (DNA base to EtBr). Then, excess CS solution (N/P ratio of 7 : 1) was added to the stained DNA solution. The fluorescence intensity of the solution was recorded on a fluorometer with excitation and emission wavelengths 493 and 523 nm, respectively. After that, a sodium chloride solution (5M) was gradually added to the solution to increase the ionic strength of the solution. The fluorescence intensity at the same excitation and emission wavelengths at different sodium chloride concentration was recorded.

MTT assay for polymer cytotoxicity

The cytotoxicity of CS on the HeLa cells was evaluated via MTT assay. Cells were seeded at 3×10^5 cells/well in 96-well microtiter plates in complete medium, DMEM with 10% fetal bovine serum (FBS) for HeLa cells. The cells were then incubated for 24 h in a humidified atmosphere of 5% CO_2 and at a temperature of 37°C. Then, the test samples of CS/pDNA complex were added as a negative controller to the wells and fresh pDNA was added as a positive controller to the wells and left them for another 24 h under 5% CO_2 atmosphere and 37°C for incubation. The cell viability was assayed by adding 10 μL of MTT Hank's balanced salt (HBS) solution (5 mg/mL). After incubation at 37°C for another 3 h, 100 μL of Stop mix solution (20% sodium dodecyl sulfate in 50% dimethyl formamide) was added to the plate and left it for another 1 h to dissolve the obtained crystal. The absorbance of each well was measured by using a microplate reader (Stat Fax 2100, Awareness) at a test wave length of 550 nm.

DNase I digestion assay

The digestion of naked pDNA and CS/pDNA complexes against DNase I (1 unit/ μL , Takara, Japan) was assayed in 2 mL of 10 mM phosphate buffered saline (PBS) containing 5 mM MgCl_2 at 37°C. At first, CS/pDNA complexes and naked pDNA were incubated with 10 μL of DNase I for 10 min at 37°C and then, DNase I was inactivated by adding of EDTA (ethylene diamine tetra acetate) (0.5M) followed by heating at 80°C for 2 min. The pDNA was developed on 0.8% agarose gel and stained with ethidium bromide.

RESULTS AND DISCUSSION

Determination of molecular weight and degree of deacetylation of chitosan

To determine the intrinsic viscosity of CS solution in 0.5M acetic acid/0.2M sodium acetate aqueous solution at 25°C, a plot of (η_{sp}/C) versus C was plotted. A straight line was obtained according to the Huggins equation and extrapolation of the plot to $C \rightarrow 0$ gave an intercept on the (η_{sp}/C) axis which was equal to $[\eta]$. From the graph, the value of $[\eta]$ was obtained 8.540 dL/g (as shown in Fig. 2). For the determination of $[\eta]$, it is necessary to extrapolate the (η_{sp}/C) versus C plot to infinite dilution (i.e., $C \rightarrow 0$). Because, at infinite dilution the polymer molecules in the solution contribute to viscosity discretely without mutual interfere. The MW of CS was obtained approximately 563 kDa [using eq. (1)]. The same was also determined by GPC and the MW of CS was obtained approximately 570 kDa.

The DDA of CS was determined by potentiometric titration method. In potentiometric titration, the

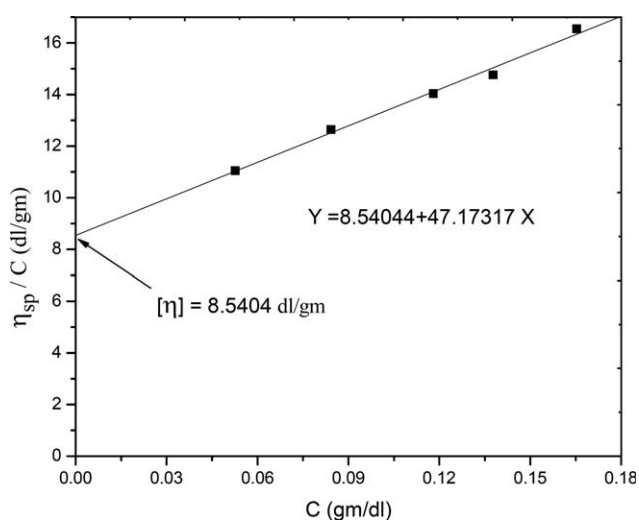


Figure 2 Typical plot of (η_{sp}/c) versus C for the determination of intrinsic viscosity $[\eta]$ of CS-0.5 (M) AcOH/0.2 (M) AcONa solvent at 25°C.

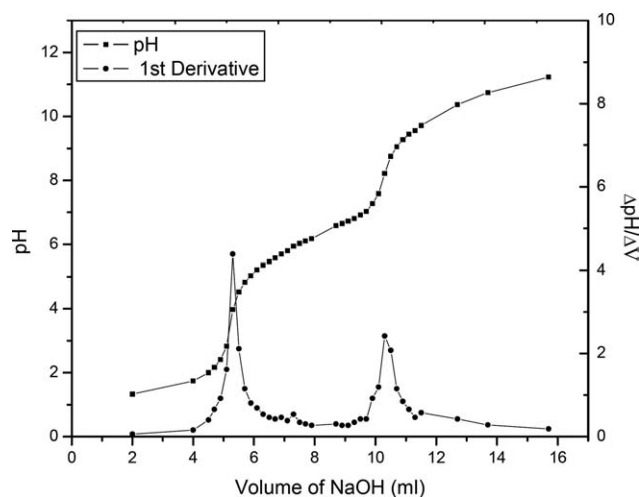


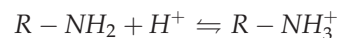
Figure 3 Potentiometric titration curve of CS and first derivative curve for the determination of two inflection points; V_1 (the equivalence point of the excess HCl) and V_2 (the equivalence point of the protonated amino groups).

value of $V_2 - V_1$ was determined from the first derivative graph of $(\Delta pH/\Delta V)$ versus volume of NaOH solution (mL) (Fig. 3). In the first derivative graph of $(\Delta pH/\Delta V)$ versus C , two peaks were observed. The first peak was observed at the point V_1 , because at this point all the excess H^+ ions in the aqueous acidic CS solution were consumed by the OH^- ions of NaOH during the titration which also corresponded to the first jump in pH of the CS solution (shown in Fig. 3). The second peak was obtained at the point V_2 due to consumption of all protonated H^+ ions of amino groups by OH^- ions of NaOH during the titration, which caused the second jump in pH of CS solution (shown in Fig. 3). By determining the value of $(V_2 - V_1)$ from the first derivative graph, the DDA of CS was obtained $\sim 83\%$ [using eq. (2)]. In Gran-type linearization method, the value of V_e was determined by extrapolating the linear titration curve of $f(x)$ versus volume of NaOH (mL) to the x -axis (Fig. 4). Here, the DDA of CS was obtained $\sim 86\%$ [using eqs. (3) and (4)].

In potentiometric titration, the titration was carried out from the pH 2 to pH 11 to determine the value of $(V_2 - V_1)$. Normally, CS precipitates from the solution after 70% degree of titration i.e., at pH > 6.0 .³⁶ Once the precipitation occurs, it reduces the concentration of CS in the solution. The precipitate may result error in the calculation of DDA by using eq. (2). Furthermore, the precipitate covers the surface of glass electrode and the response of electrode became sluggish. But, the titration was carried out up to pH 4 in the Gran-type linearization method to calculate the DDA of CS by using eq. (3).

The aqueous acidic solution (HCl aqueous solution) of CS becomes polyelectrolyte because of the

amine groups of CS protonated by the H^+ ion from the aqueous acidic solution. In the ionization state, the equilibrium reaction may be described as:



Therefore, the dissociation constant of protonated CS ($R - NH_3^+$) may be defined as:

$$K_a = \frac{[R - NH_2][H^+]}{[R - NH_3^+]} \quad (6)$$

In the above equation, it is found that the dissociation constant of protonated CS depends on the concentration of H^+ ion. So, it is necessary to calculate the concentration of H^+ ion. The ionic strength of titrate (NaOH solution) was kept at 0.1 during the whole titration process because the concentration of H^+ ion can be converted into activity of H^+ ion, α_H^+ ($\alpha_H^+ = 10^{-pH}$) by the following relationship³⁷:

$$[H^+] = \alpha_H^+ \times 10^{0.08} \quad (7)$$

As the dissociation constant of protonated CS depends on the concentration of H^+ ion, the DDA calculation of CS by the linear potentiometric titration method [eq. (3)] is more authentic than that of the Gran-type linearization method [eq. (2)].

Formation of CS/pDNA complex

The formation of complex between two oppositely charged polyelectrolyte partners can be characterized by the electrophoretic retardation bands in agarose gel. The neutralization and the increase in molecular size of the complex results in the

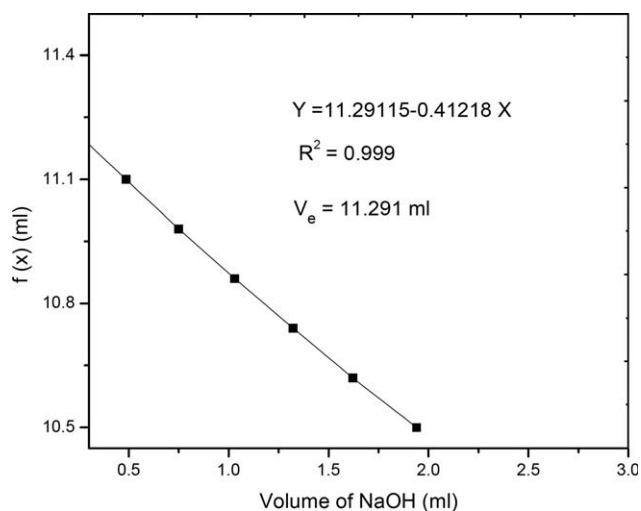


Figure 4 Plot of $f(x)$ versus volume of NaOH in different pH region for the determination of V_e by extrapolation of the graph to the Y -axis.

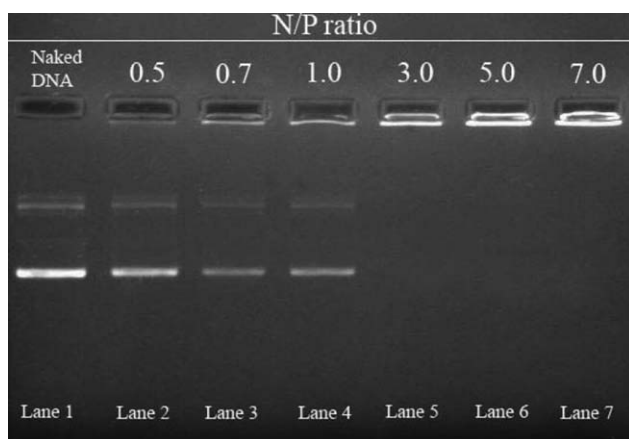


Figure 5 Gel electrophoresis shift assay of DNA and CS/pDNA complexes at various charge ratios. Samples were subjected to 0.8% agarose gel electrophoresis. The samples were as follows: Lane 1, plasmid DNA alone; Lane 2, 0.5 : 1; Lane 3, 0.7 : 1; Lane 4, 1 : 1; Lane 5, 3 : 1; Lane 6, 5 : 1; and Lane 7, 7 : 1.

complete retardation of pDNA migration towards the anode in the electric field.³⁸ One interesting feature of CS is its cationic character because of the presence of primary amine group in its structure (Fig. 1). Therefore, CS is expected to form complexes by electrostatic interaction with pDNA due to its negative charge. Figure 5 shows the influence of charge ratios on DNA condensation by CS. Free DNA alone was shown in Lane 1. The results indicated that the electrophoretic mobility of DNA was retarded with increasing the N/P ratio i.e., with increasing amount of CS, and even remained at the top of the gel at charge ratio of 3–7 (Lane 5–7). This result suggested that CS formed complexes completely with DNA at those ranges.

As the MW of CS is high, the number of primary nitrogen atom (for a fixed DDA value, here 86%) in the CS chain will also be high. Therefore, at a certain pH value (pH 5.5), the positive charge will be high due to the protonation of the primary amine groups, which help to condense the negatively charged pDNA more efficiently than that of low MW CS. So, it may be expected that the size of the self-assembled complex will be low.

Particle sizes, morphology and zeta potential of CS/pDNA complexes

Proper particle size and positive surface charge of polycation/DNA complexes are important for cell uptake and efficient transfection. Endocytosis by many types of mammalian cells is limited to particles less than about 150 nm in diameter.³⁹ Although, spleen, bone marrow, tissues of the reticulo-endothelial system and liver permit relatively free passage of materials without size restrictions,

up to 100 nm due to their sinusoidal endothelial structure.⁴⁰ Therefore, it is necessary to characterize the size and morphology of polyplexes, because these properties play very important role in the transfection of exogenous genes into target cells and expression of therapeutic genes. The size and distribution of nonviral vector/DNA complexes can be determined efficiently by DLS. Figure 6 shows the mean diameters of CS/DNA complexes at the charge ratios of 1 : 1, 3 : 1, 5 : 1, and 7 : 1, respectively, by means of DLS. These results show that CS can condense plasmid DNA to form nanometer-scale particles at different charge ratios from 1 : 1 to 7 : 1. But, CS forms efficient nanoparticle with DNA at the charge ratio of 3 : 1 with mean diameter within 150 nm, which is suitable for gene therapy. As the charge ratio increases from 1 : 1 to 3 : 1, the mean diameter decreases slightly from 132 to 115 nm. This can be explained by the fact that with an increase in positive charge, the electrostatic interaction increases accordingly and results in decreased size of the complex. When the charge ratio of the complexes further increases, the mean diameter of CS/DNA complexes also increases due to the fact that the exchange repulsion induced by excessive positive charge gains predominance over the electrostatic interaction.

To study the influence of polymer on size and shape of the complexes formed with plasmid DNA, we performed AFM experiment. Transmission electron microscopy (TEM) is frequently used to characterize polycation/DNA complexes, but AFM has some advantage over the TEM. The AFM image can

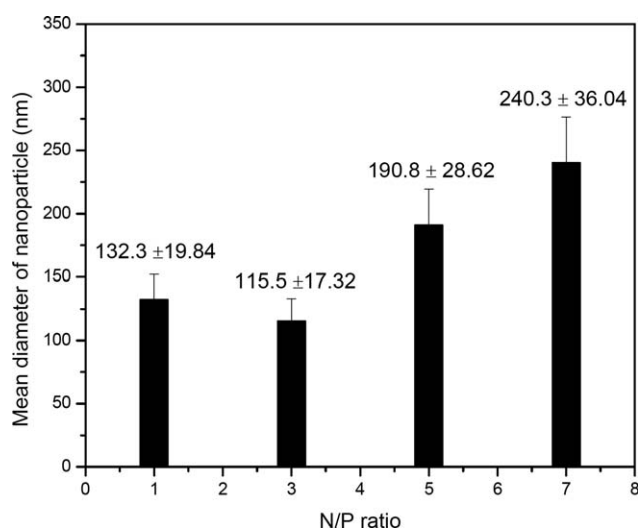


Figure 6 Mean diameter of CS/pDNA complexes at various charge ratios. The particle size of the complexes was measured by DLS. The DLS measurement was carried out by means of an argon ion laser system tuned at 514 nm. The intensity of autocorrelation was measured at a scattering angle (θ) of 173° with a Nano ZS (Malvern Instrument, UK) digital autocorrelator at 37°C.

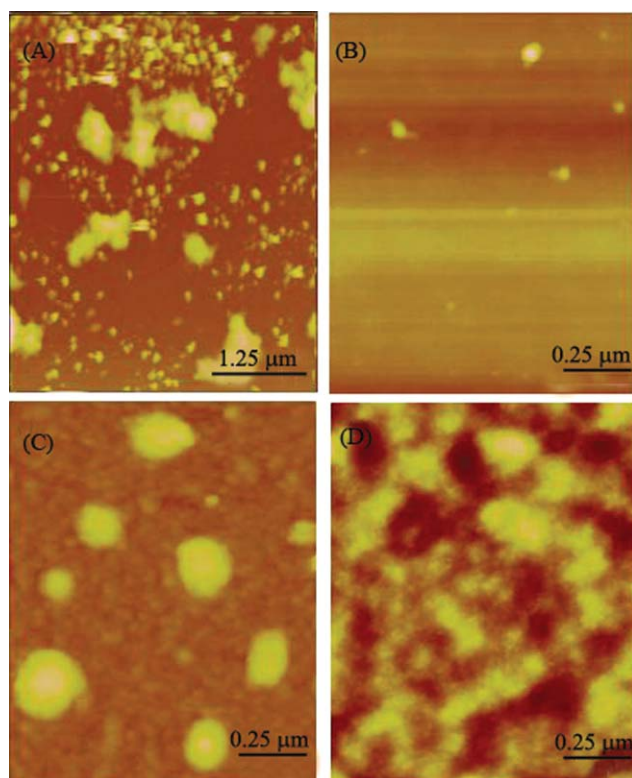


Figure 7 AFM images of CS (A) and CS/pDNA complexes at different charge ratios of 3 : 1 (B), 5 : 1 (C), and 7 : 1 (D). [Color figure can be viewed in the online issue, which is available at wileyonlinelibrary.com.]

be performed on a wide range of surfaces and in different environments as well as it can be performed without staining, e.g., with zinc uranyl acetate, or other contrast enhancement. Figure 7 shows the AFM images of CS as well as CS/DNA complexes at the charge ratio of 3 : 1, 5 : 1, and 7 : 1. The size and surface morphology of the complexes obtained from the figure demonstrate that the nanoparticles are spherical in shape with diameter varying from 60 to 100 nm [Fig. 7(B)], 140 to 195 nm [Fig. 7(C)], and 180 to 250 nm [Fig. 7(D)], which are coincident with the measurements of DLS. Moreover, the SEM image of CS/pDNA complex at the charge ratio of 3 : 1 (Fig. 8) also demonstrates that the nanoparticles are spherical in shape with the diameter within 100 nm, which is also in agreement with the DLS as well as AFM experiments. Previous studies showed that the mean diameter of self-assembled CS/pDNA complex was around 100 nm.⁴¹ Illum et al.⁴² also prepared CS/pDNA nanoparticles ranging from 20 to 500 nm.

The zeta potential of CS/DNA complexes at different charge ratios is shown in Figure 9. CS/DNA complexes at the charge ratios from 0.5 to 1, where the complexes could not be formed completely, showed negative zeta potentials, whereas the ones at higher charge ratios that is, above the charge ratio of 1 showed gradual increase of zeta potentials with

raising the charge ratios. Complete shielding of DNA (–) charge occurred in the vicinity of charge ratio of 3 and no significant difference of zeta potential was observed between the charge ratios of 3–7.

It was reported that slightly positive zeta potential resulted in the best transfection efficiency.⁴³ Therefore, CS/pDNA complex above charge ratio of 1 is thought to be profitable for the gene transfer into cells.

Stability of CS/pDNA complex

In the successful gene therapy, especially in case of intravenous injection, a long circulation time for polycation/DNA complex is an important and fundamental factor for reaching the target cells. The dispersive stability of CS/pDNA complexes was observed using turbidity measurements. In the turbidity measurements, the increase in turbidity indicates self-aggregation and the decrease reflects precipitation during the time course of incubation. Figure 10 shows the turbidity of CS/pDNA complexes at different charge ratios. The results showed that the turbidity of all CS/pDNA complexes slightly decreased at day 1. The turbidity of the complexes at the charge ratios of 0.5 : 1 and 1 : 1 sharply increased at day 2, and then it gradually increased with time. But, the turbidity of the complexes at the charge ratios from 3 to 7 remained constant after day 2. This result indicates that self-aggregation of DNA occurred at low concentration of CS. The most enhanced stability of the complexes was obtained at higher charge ratio i.e., from the charge ratio 3 : 1, indicating the prevention of self-aggregation occurred due to appropriate charge

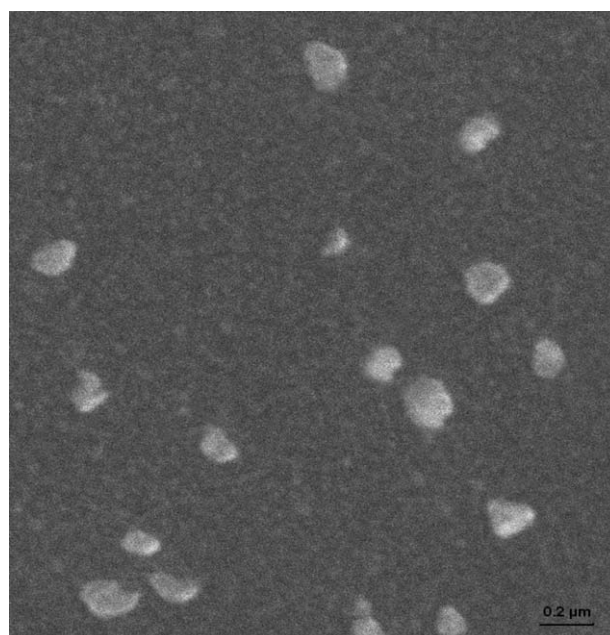


Figure 8 Typical SEM image of CS/pDNA complex at the charge ratio of 3 : 1.

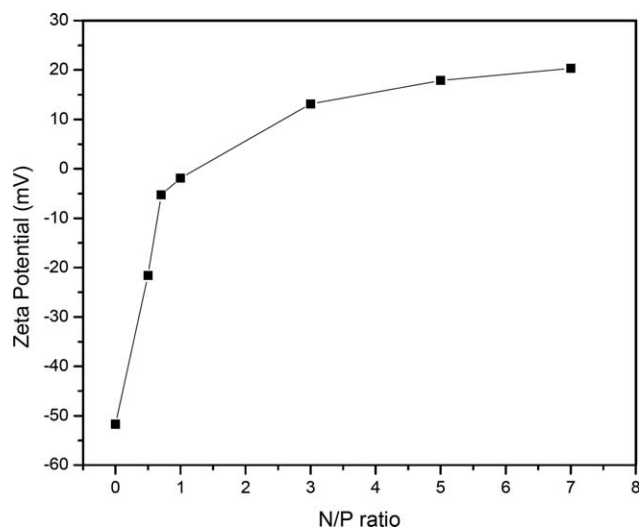


Figure 9 Zeta potential of CS/pDNA complexes at the different charge ratios.

repulsion of CS. Therefore, it is expected that the CS/pDNA complexes above the charge ratio of 3 : 1 will be effective for successful gene therapy.

Effect of ionic strength on CS/DNA complex

In complex coacervation method, CS and DNA form CS/DNA nanoparticles. The cationic characteristic of CS is a crucial parameter for complex formation. CS consists of 2-aminoglucoside group in its repeating unit. Since, the pK_a value of amino group in these repeating unit is 6.5, hence majority of amino groups (>90%) are protonated at pH 5.5 and solubilizing the CS in acidic solution. But, at physiological pH, most of the positive charges would be neutralized,

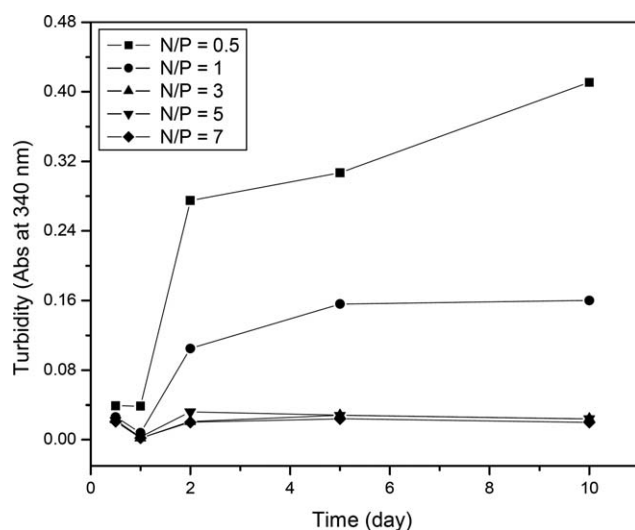


Figure 10 Stability of CS/pDNA complexes. Turbidity of CS/pDNA complexes at various charge ratios with increasing incubation period.

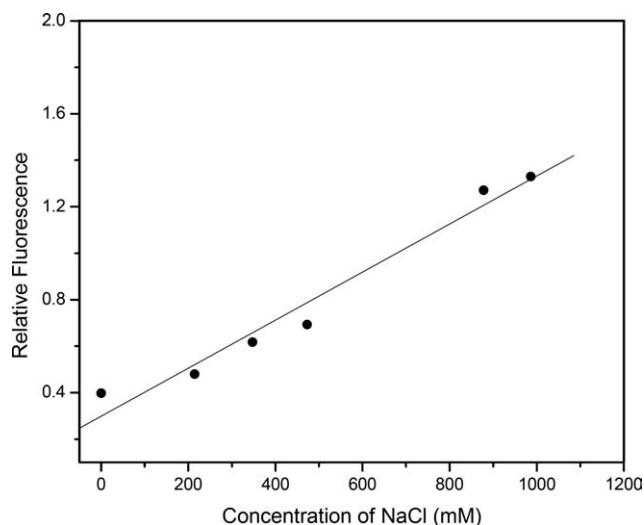


Figure 11 Effect of ionic strength on the interaction between CS and DNA. The fluorescence intensity was recorded at excitation and emission wavelengths of 493 and 523 nm, respectively, at different concentration of NaCl.

and the hydrophobic CS becomes insoluble. This unique property reveals that CS can only form nanoparticle with DNA at low pH and could remain stable at physiological pH.

The influence of ionic strength on the interaction between CS and DNA was examined by competitive binding assay using an ethidium bromide (EtBr) stained plasmid DNA. EtBr stained DNA fluoresced strongly when EtBr occupied the effective binding sites on DNA and binds with DNA. When CS was

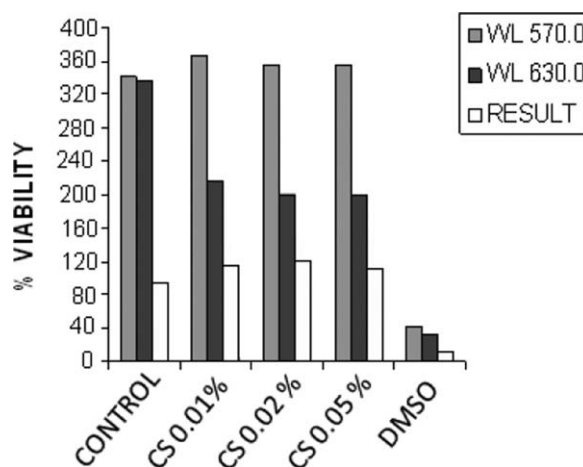


Figure 12 Cytotoxicity of CS against HeLa cells. HeLa cells were seeded at a density of 3×10^5 cells/well in 96-well microtiter plates. CS/pDNA nanoparticles were added and the samples were incubated for 24 h at 37°C. The mixture was replaced with 10 μ L of MTT dye solution and after 3 h of incubation, crystals were dissolved with DMSO. The absorbance was read at 540 nm by use of a microplate reader.

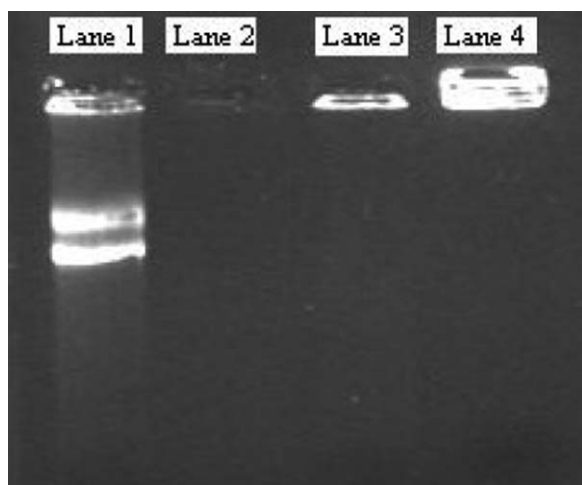


Figure 13 DNase I digestion assays of CS/pDNA complexes. Naked pDNA and CS/pDNA complexes are treated with 0.1 U of DNase I. Samples were subjected to 0.8% agarose gel electrophoresis. The samples were as follows: Lane 1, naked pDNA; Lane 2, naked pDNA treated with DNase I; Lane 3, CS/pDNA complex at N/P ratio of 3 treated with DNase I; and Lane 4, CS/pDNA complex at N/P ratio of 5 treated with DNase I.

added to the solution, the fluorescence intensity of the solution decreased because the positive charge of CS competed with EtBr for binding with DNA. When maximum binding occurs between CS and DNA, then the fluorescence intensity reached a plateau at the charge ratio of 3 : 1 (data not given). Above this threshold charge ratio, i.e., at the charge ratio of 7 : 1, sodium chloride solution was added to increase the ionic strength in the solution to measure the ability of the salt to shield the interactions between CS and DNA. As shown in Figure 11, as the concentration of NaCl increases, the relative ethidium bromide fluorescence increases, suggesting that binding affinity of CS for DNA decreases. The linear increase of fluorescence with increasing the NaCl concentration indicates that charge shielding due to higher ionic strength adversely affects the binding. This result demonstrated a predominantly electrostatic interaction between CS and DNA.

Cytotoxicity of chitosan

The MTT assay was carried out to observe the cytotoxicity of CS on the HeLa cell lines. The effect of CS on cell viability was measured by applying different concentrations (0.01–0.05%) of CS. CS/pDNA complexes were added to HeLa cells and incubated for 4 h. After incubation, cell viability was determined by MTT assay. Figure 12 shows the cytotoxicity of CS at various concentrations against HeLa cells. No significant decrease in cell viability was observed

in CS with the concentration from 0.1 mg/mL to 0.5 mg/mL.

It is found that the cytotoxicity of CS does not vary significantly with varying the concentration of CS from 0.5 to 0.1 mg/mL. Huang et al.⁴⁴ showed that CS exhibits significant cytotoxicity above the concentration of 0.741 mg/mL and they also showed that the cytotoxicity did not depend extensively on the MW of CS. The cytotoxicity of cationic polymer was directly related to the surface charge density of polymer.⁴⁵ The number of primary amino groups of cationic polymers was important⁴⁶ because the surface charge density of polymer was related to the number of primary amino groups. Although, the three dimensional arrangement of the cationic residue of polymer is an important factor for cytotoxicity. CS with a higher DDA value as well as higher MW have unmitigated conformation due to the charge repulsion, which may allow them to bind more easily with the cell membrane than the coiled CS with lower DDA.

Resistance to DNase I digestion

Protection of plasmid DNA by CS from DNase degradation was examined using DNase I as a model enzyme (Fig. 13). When incubated with DNase I at 37°C, naked plasmid DNA showed complete degradation (Lane 2) within 1 h, whereas the plasmid DNA in the CS/pDNA complex at the charge ratios of 3 and 5 after the same treatment remained intact (Lanes 3 and 4). Therefore, the DNase I digestion assay suggests that CS can protect the pDNA effectively against DNase I degradation.

CONCLUSION

In this work, nanoparticles of CS/pDNA were prepared by complex coacervation process under defined conditions. It was found that higher molecular weight CS showed good DNA binding ability at very low concentration with the formation of nanoparticles within 100 nm. The physicochemical properties of the complexes were also examined. It was found that the interaction between CS and DNA was completely electrostatic and the zeta potential of the complexes was positive at higher charge ratio. It was also found that the CS/DNA complexes were quite stable at higher charge ratio up to few days and CS protected the DNA from enzyme effectively. Therefore, it is expected that CS/pDNA complex will be suitable for successful gene therapy.

We are grateful to Prof. D. J. Chattopadhyay, Professor of Biotechnology Pro VC (Academic), for his valuable comments and suggestions and also thankful to Dr. A. Mukherjee, Professor of Pharmaceutical, University of Calcutta for characterization by DLS in his laboratory.

References

1. Gingrich, J. R.; Chauhan, R. D.; Steiner, M. *Curr Oncol Rep* 2001, 3, 438.
2. Fanning, G.; Amado, R.; Symonds, G. *J Gene Med* 2003, 5, 645.
3. Rowland, R. CNN Medical Unit 2001, April 10. Available at: http://articles.cnn.com/2001-04-10/health/alzheimer.surgery_1_gene-therapy-brain-cells-amyloid?_s=PM:HEALTH.
4. Hally, Z. *Science Daily* 2007, June 25. Available at: <http://www.sciencedaily.com/releases/2007/06/070622101037.htm>.
5. Brugada, R.; Roberts, R. *Expert Opin Ther Pat* 2000, 10, 1385.
6. Kean, T.; Roth, S.; Thanou, M. *J Controlled Release* 2005, 103, 643.
7. Wong, K.; Sun, G. B.; Zhang, X. Q.; Dai, H.; Liu, Y.; He, C. B.; Leong, K. W. *Bioconjugate Chem* 2006, 17, 152.
8. Mansouri, S.; Lavigne, P.; Corsi, K.; Benderdour, M.; Beaumont, E.; Fernandes, J. C. *Eur J Pharm Biopharm* 2004, 57, 1.
9. Lee, H.; Kim, T. H.; Park, T. G. *J Controlled Release* 2002, 16, 147.
10. Wagner, E.; Ogris, M.; Zauner, W. *Adv Drug Delivery Rev* 1998, 30, 97.
11. Wightman, L.; Kircheis, R.; Rossler, V.; Carotta, S.; Ruzicka, R.; Kursa, M.; Wagner, E. *J Gene Med* 2001, 3, 362.
12. Zhang, X. Q.; Wang, X. L.; Huang, S. W.; Zhuo, R. X.; Liu, Z. L.; Mao, H. Q.; Leong, K. W. *Biomacromolecules* 2005, 6, 341.
13. Wang, J.; Zhang, P. C.; Lu, H. F.; Ma, N.; Wang, S.; Mao, H. Q.; Leong, K. W. *J Controlled Release* 2002, 83, 157.
14. Lynn, D. M.; Langer, R. *J Am Chem Soc* 2000, 122, 10761.
15. Harpe, V.; Petersen, A.; Li, H. Y.; Kissel, T. *J Controlled Release* 2000, 69, 309.
16. Boussif, O.; Lezoualch, F.; Zanta, M. A.; Mergny, M. D.; Scherman, D.; Demeneix, B.; Behr, J. P. *Proc Natl Acad Sci USA* 1995, 92, 7297.
17. Mao, H. Q.; Roy, K.; Troung-Le, V. L.; Janes, K. A.; Lin, K. Y.; August, J. T.; Leong, K. W. *J Controlled Release* 2001, 70, 399.
18. Park, I. K.; Kim, T. H.; Park, Y. H.; Shin, B. A.; Choi, E. S.; Chowdhury, E. H.; Akaike, T.; Cho, C. S. *J Controlled Release* 2001, 76, 349.
19. Kim, T. H.; Ihm, J. E.; Choi, Y. J.; Nah, J. W.; Cho, C. S. *J Controlled Release* 2003, 93, 389.
20. Koping-Hoggard, M.; Tubulekas, I.; Guan, H.; Edwards, K.; Nilsson, M.; Varum, K. M.; Artursson, P. *Gene Ther* 2001, 8, 1108.
21. Dong, J. M.; Leong, K. W. *Adv Drug Deliv Rev* 2006, 58, 487.
22. Onishi, H.; Machida, Y. *Biomaterials* 1999, 20, 175.
23. Rao, S. B.; Sharma, C. P. *J Biomed Mater Res* 1997, 34, 21.
24. Aspden, T. J.; Mason, J. D.; Jones, N. S. *J Pharm Sci* 1997, 86, 509.
25. Dodane, V.; Vilivalam, V. D. *Pharm Sci Technol Today* 1998, 1, 246.
26. Ishii, T.; Okahata, Y.; Sato, T. *Biochim Biophys Acta* 2001, 1514, 51.
27. MacLaughlin, F. C.; Mumper, R. J.; Wang, J. J.; Tagliaferri, J. M.; Gill, I.; Hinchcliffe, M.; Rolland, A. P. *J Controlled Release* 1998, 56, 259.
28. Lillo, L. F.; Matsuhira, B. *Carbohydr Polym* 1997, 34, 397.
29. Kim, T. H.; Park, I. K.; Nah, J. W.; Choi, Y. J.; Cho, C. S. *Biomaterials* 2004, 25, 3783.
30. Erbacher, P.; Zou, S.; Bettinger, T.; Steffan, A. M.; Remy, J. S. *Pharm Res* 1998, 15, 1332.
31. Philippova, O. E.; Volkov, E. V.; Sitnikova, N. L.; Khokhlov, A. R.; Desbrieres, J.; Rinaudo, M. *Biomacromolecules* 2001, 2, 483.
32. Kiang, T.; Wen, J.; Lim, H. W.; Leong, K. W. *Biomaterials* 2004, 25, 5293.
33. Chebotok, E. N.; Novikov, V. Y.; Konovalova, I. N. *Russ J Appl Chem* 2007, 80, 1753.
34. Ke, H.; Chen, Q. *Huaxue Tongbao* 1990, 10, 44.
35. Jiang, X.; Chen, L.; Zhong, W. *Carbohydr Polym* 2003, 54, 457.
36. Domard, A.; Rinaudo, M. *Int J Biol Macromol* 1983, 5, 49.
37. Ingman, L. F.; Still, E. *Talanta* 1966, 13, 1431.
38. Lee, M.; Nah, J. W.; Kwon, Y.; Koh, J. J.; Ko, K. S.; Kim, S. W. *Pharm Res* 2000, 18, 427.
39. Guy, J.; Drabek, D.; Antoniou, M. *Mol Biotechnol* 1995, 3, 237.
40. Seymour, L. W. *Crit Rev Ther Drug Carrier Syst* 1992, 9, 135.
41. Mansouri, S.; Lavigne, P.; Corsi, K.; Benderdour, M.; Beaumont, E.; Fernandes, J. C. *Eur J Pharm Biopharm* 2003, 57, 1.
42. Illum, L.; Jabbal-Gill, I.; Hinchcliffe, M.; Fisher, A. N.; Davis, S. S. *Adv Drug Deliv Rev* 2001, 51, 81.
43. Kim, J. S.; Kim, B. I.; Maruyama, A.; Akaike, T.; Kim, S. W. *J Controlled Release* 1998, 53, 175.
44. Huang, M.; Khor, E.; Lim, L. Y. *Pharm Res* 2004, 21, 344.
45. Chang, S. W.; Westcott, J. Y.; Henson, J. E.; Voelkel, N. F. *J Appl Physiol* 1932 1987, 62.
46. Ekrami, H. M.; Shen, W. C. *J Drug Target* 1995, 2, 469.